DOI: 10.51984/SUCP.V4I3.4107

وقائع مؤتمرات جامعة سبها
Sebha University Conference Proceedings
Confrence Proceeeding homepage: http://www.sebhau.edu.ly/journal/CAS

Numerical Investigation of the Time-Dependent Schrödinger Equation Via Finite Difference Approach

Dalal Y. Saad[1] & *Fawzi A. Ikraiam[2]

[1]Physics Department, Faculty of Science, Omar Al-Mukhtar University, EL-Beida, Libya
[2]Physics Research Group, Physics Department, Faculty of Science, University of Benghazi, Benghazi, Libya

Keywords:
Time-dependent Schrödinger Equation (TDSE)
Finite Difference Method
Numerical Simulation
Step Barrier
MATLAB

ABSTRACT

This paper presents a conceptually straightforward, accurate, and efficient numerical approach for obtaining solutions to the time-dependent Schrödinger equation (TDSE), utilizing the Finite Difference Method (FDM). The methodology employs a forward difference scheme for temporal derivatives and a second-order central difference scheme for spatial derivatives, with the computational framework implemented in MATLAB. The efficacy of the proposed method is rigorously demonstrated through simulations of an electron wave packet in various scenarios. Key findings include the confirmation of fundamental quantum principles, such as the Heisenberg Uncertainty Principle and the conservation of total energy (expectation value) throughout system evolution. Analysis of wave packet interactions with both attractive and repulsive step barriers reveal phenomena of dispersion, probabilistic reflection, and transmission, with the total probability consistently conserved. Furthermore, the dynamics of electron wave packets in uniform electric fields (accelerating, retarding, and zero-field conditions) are explored, illustrating energy transformations and providing insights into their behaviour in comparison to classical predictions. These simulations collectively underscore the robustness and versatility of the FDM approach, which is readily extensible to higher dimensions and diverse time-dependent applications, thereby contributing to a deeper computational understanding of quantum mechanical systems.

التحقيق العددي لمعادلة شرودنغر المعتمدة على الزمن عبر منهج الفروق المحدودة

دلال يحي سعد[1] و *فوزي عبدالكريم اكريم[2]

[1]قسم الفيزياء، كلية العلوم، جامعة عمر المختار، البيضاء، ليبيا
[2]مجموعة أبحاث الفيزياء، قسم الفيزياء، كلية العلوم، جامعة بنغازي

الكلمات المفتاحية:
الحاجز المتدرج
المحاكاة العددية
طريقة الفروق المحدودة
ماتلاب
معادلة شرودنغر المعتمدة على الزمن

الملخص

يُقدم هذا البحث منهجًا عدديًا مباشرًا ودقيقًا وفعالًا للحصول على حلول لمعادلة شرودنغر المعتمدة على الزمن (TDSE)، وذلك باستخدام طريقة الفروق المحدودة (FDM) .تستخدم المنهجية مخطط الفروق الأمامية للمشتقات الزمنية ومخطط الفروق المركزية من الرتبة الثانية للمشتقات المكانية، وقد تم تطبيق الإطار الحسابي في برنامج MATLAB .تم إثبات فعالية الطريقة المقترحة بدقة من خلال محاكاة حزمة موجية إلكترونية في سيناريوهات مختلفة. تشمل النتائج الرئيسية تأكيد المبادئ الكمومية الأساسية، مثل مبدأ هايزنبرغ لعدم اليقين والحفاظ على الطاقة الكلية (القيمة المتوقعة) خلال تطور النظام. يكشف تحليل تفاعلات حزمة الموجة مع حواجز خطوية جاذبة ونافره عن ظواهر الانتشار والانعكاس الاحتمالي والانتقال، مع الحفاظ على الاحتمال الكلي بشكل ثابت. علاوة على ذلك، تم استكشاف ديناميكيات حزم الموجات الإلكترونية في المجالات الكهربائية المنتظمة (ظروف التسريع والتباطؤ والمجال الصفري)، مما يوضح تحولات الطاقة ويقدم رؤى حول سلوكها مقارنة بالتنبؤات الكلاسيكية. تؤكد هذه المحاكاة مجتمعةً على قوة وتنوع منهج FDM ، الذي يمكن توسيعه بسهولة ليشمل أبعادًا أعلى وتطبيقات متنوعة تعتمد على الزمن، وبالتالي يساهم في فهم حسابي أعمق للأنظمة الميكانيكية الكمومية.

*Corresponding author:
E-mail addresses: fawzi.ikraiam@omu.edu.ly, (D. Y. Saad) dalal.saad@omu.edu.ly
Article History : Received 20 February 2025 - Received in revised form 01 September 2025 - Accepted 07 October 2025

1. Introduction

The solution of the time-dependent Schrödinger equation (TDSE) is vital in many fields of physics and chemistry. In particular, to understand how atoms, molecules, and materials react in the presence of time-varying electromagnetic fields, in atomic collisions, or to different internal and external forces. Given the vast length and time scales over which nanoscale physical systems evolve, efficient computational methods are indispensable [Schneider, 2005]. Unlike its time-independent counterpart, which describes stationary states, the TDSE allows modelling dynamic processes such as electron transitions, chemical reactions, and the interaction of matter with light. This capability is crucial for phenomena like ultrafast spectroscopy, where scientists probe molecular changes on femtosecond timescales, and for the development of new materials with tailored optical or electronic properties. Efficient numerical solutions to TDSE are fundamental to much of atomic-scale physics today. This includes understanding phenomena like how electrons and atoms scatter off targets, intense lasers interaction with matter, and the precise optical control of energy in atoms and molecules. It is also crucial for generating quantum solitons and vortices in Bose-Einstein condensates; a problem that mirrors the propagation of light pulses in nano-structured optical fibers. In present-day research, the TDSE is indispensable for simulating complex quantum phenomena, from designing novel catalysts to understanding quantum computing. For instance, in materials science, it helps predict how new semiconductors will behave under external fields, guiding the creation of more efficient solar cells or transistors. The computational power now available allows for increasingly accurate numerical solutions to the TDSE, making it a cornerstone for predicting and manipulating the quantum world at an unprecedented level of detail. The TDSE is, thus, a fundamental equation in quantum mechanics to describe the progression of the wavefunction over time. Its numerical solution is essential for simulating various quantum phenomena, particularly those involving ultrafast dynamics and attosecond physics. TDSE simulations are also used in materials design, quantum chemistry, and even have emerging applications in quantum computing. Hence, this paper presents a numerical approach for solving the TDSE, emphasizing conceptual simplicity, accuracy, and computational efficiency. The effectiveness of this method is demonstrated through simulations of a quantum particle confined within a one-dimensional square well potential. The algorithm is explicit and meticulously outlines the computational steps, ensuring clarity and reproducibility. A key advantage of this methodology is its inherent extensibility, allowing for straightforward generalization to quantum systems with higher spatial dimensions. Furthermore, the method proves adaptable to diverse time-dependent applications, facilitating the independent and accurate calculation of both the real and imaginary components of the wave function. The robustness and precision of the algorithm are thoroughly validated through several illustrative examples [1-8].

2. Theoretical Framework and Numerical Methodology

Solving the TDSE numerically involves converting continuous variables like position (r) and time (t) into discrete points. Boundary conditions, which define the wavefunction's behavior at specific spatial locations, are incorporated by forcing the solution to meet these conditions at those points. For instance, with finite difference methods, the wavefunction's values at these boundaries must be set to ensure a determined solution. Similarly, when using function space discretization, the chosen basis set is designed to inherently satisfy these conditions. Initial conditions for time are handled by setting the wavefunction's state at the starting time. As the system evolves, it is often necessary to dynamically adjust the grid or basis set to exhibit the wavefunction's changes. The time steps themselves might also need to vary considerably throughout the simulation [6-7].

2.1 The Time-Dependent Schrödinger Equation

The dynamics of a non-relativistic quantum mechanical particle of mass m in one spatial dimension (1D) are governed by the time-dependent Schrödinger equation (TDSE) given as [8]:

$$i\hbar\frac{\partial\psi(x,t)}{\partial t} = \left[-\frac{\hbar^2}{2m}\frac{\partial^2\psi(x,t)}{\partial x^2} + U(x,t)\right] \quad \psi(x,t) \qquad (1)$$

where: $U(x,t)$ is the time-dependent potential energy function for the system, $\psi(x, t)$ is the complex wave function and $\hbar$ is the reduced Planck constant.

The wave function $\psi(x, t)$ is a complex-valued probability amplitude, such that $|\psi(x, t)|^2$ represents the probability density of finding the particle at position x at time t. For numerical solutions, appropriate initial conditions $\psi(x, 0)$ and boundary conditions, such as $\psi(x, t) = 0$ at infinite potential walls, must be specified.

2.2 Discretization Scheme

To solve the wave function (Ψ) partial differential equation, since it involves spatial and temporal evolution, it is discretized to enable numerical computation. The continuous spatial and temporal domains are discretized into a finite grid. The spatial domain extents from x_{min} to x_{max} and is divided into N_x discrete points, resulting in a spatial step size, given by $\Delta x = (x_{max} - x_{min})/(N_x - 1)$, to correctly account for the number of intervals. The grid points are then defined as $x_j = x_{min} + j\Delta x$, where j ranges from 0 to N_x-1. Then, $\Psi(x_j, t_n)$ signifies a continuous wave function being approximated by a value at a specific spatial grid point x_j and a specific time step t_n. This discretization process is the first step in applying numerical methods such as Finite Difference Method (FDM), where the derivatives in the continuous equations are replaced by finite difference approximations using the values at adjacent grid points. By discretizing the domain, a continuous problem that might be difficult or impossible to solve analytically is transformed into a system of algebraic equations that can be solved computationally. The accuracy of the numerical solution often depends on the chosen step sizes (Δx and Δt), where smaller step sizes usually lead to more accurate results. Similarly, the temporal domain is discretized with a time step Δt, such that $t_n = n\,\Delta t$, where n from 0 to N_t-1 [9-18].

2.3 Finite Difference Approximation

The numerical solution of the TDSE is achieved through the application of the Finite Difference Method (FDM). This approach involves approximating the partial derivatives in Equation (1) using finite difference formulae. The first-order partial derivative with respect to time is approximated using a forward difference scheme as follows [15]:

$$\frac{\partial\psi}{\partial t} \approx \frac{\psi_j^{n+1} - \psi_j^n}{\Delta t} \qquad (2)$$

The second-order partial derivative with respect to space is approximated using a central difference scheme, which provides second-order accuracy in space as follows:

$$\frac{\partial^2\psi}{\partial x^2} \approx \frac{\psi_{j+1}^n - 2\,\psi_j^n + \psi_{j-1}^n}{(\Delta t)^2} \qquad (3)$$

2.4 Separation of Real and Imaginary Components

An essential step in formulating an explicit numerical algorithm for the TDSE is to decompose the complex wave function into its real, $R(x, t)$, and imaginary, $I(x, t)$, parts as follows:

$$\psi(x, t) = R(x, t) + iI(x, t) \qquad (4)$$

Substituting this decomposition into the TDSE (Equation 1) and equating the real and imaginary parts of the resulting equation yields a coupled system of two real-valued partial differential equations [13]:

$$-\hbar\frac{\partial I}{\partial t} = -\frac{\hbar^2}{2m}\frac{\partial^2 R}{\partial x^2} + U(x,t)R \quad (5)$$

$$\hbar\frac{\partial R}{\partial t} = -\frac{\hbar^2}{2m}\frac{\partial^2 I}{\partial x^2} + U(x,t)I \quad (6)$$

2.5 The Numerical Algorithm

By substituting the finite difference approximations from Section 2.3 into the coupled real and imaginary component equations (Section 2.4), an explicit algorithm for the time evolution of the wave function can be derived. At each grid point (x_j, t_n), the real and imaginary components at the next time step, R_j^{n+1} and I_j^{n+1}, can be explicitly calculated from values at the current time step n and their spatial neighbours:

$$R_j^{n+1} = R_j^n - \frac{\Delta t}{\hbar}\left[-\frac{\hbar^2}{2m}\frac{I_{j+1}^n - 2I_j^n + I_{j-1}^n}{(\Delta x)^2} + U(x_j, t_n)I_j^n\right] \qquad (7)$$

$$I_j^{n+1} = I_j^n - \frac{\Delta t}{\hbar}\left[-\frac{\hbar^2}{2m}\frac{R_{j+1}^n - 2R_j^n + R_{j-1}^n}{(\Delta x)^2} + U(x_j, t_n)R_j^n\right] \quad (8)$$

This explicit scheme is straightforward to implement. However, it is essential to note that explicit finite difference methods for the TDSE, particularly the Forward-Time Central-Space (FTCS) scheme implied here, are conditionally stable. A stability criterion, often related to the Courant-Friedrichs-Lewy (CFL) condition, must be satisfied for the numerical solution to remain bounded. For the TDSE, this typically imposes a strict upper limit on the time step Δt in relation to the spatial step Δx as given by:

$$\Delta t \leq \frac{m(\Delta x)^2}{2\hbar}$$

This condition will need to be carefully considered during simulations to ensure accurate and stable results [19].

2.6 The MATLAB Code Implementation

The numerical solution of the TDSE, based on the finite difference approximations, was implemented in a custom-built MATLAB code. This programming environment was selected for its robust numerical capabilities and extensive library functions, which facilitate efficient matrix operations and data visualization essential for quantum mechanical simulations. This program methodically translates the discretized FDM equations into an iterative computational scheme. It begins by defining the 1D spatial grid with a resolution of Δx and establishing discrete time steps of Δt. At each subsequent time step, the code computes the wave function's new state by applying the finite difference relations to the wave function from the previous step, while dynamically incorporating the chosen potential energy function (e.g., free space, step barrier, or uniform electric field). Beyond solving for the wave function, the code is programmed to calculate and track key quantum observables, including the probability density, expectation values for position, momentum, kinetic energy, potential energy, and their respective uncertainties. Finally, the code generates comprehensive graphical outputs, allowing for the visualization of the wave packet's temporal evolution and the clear demonstration of the simulated quantum phenomena. All simulated results presented in the subsequent sections of this paper, including the temporal dynamics of the quantum particle within a step barrier structure, were generated using this custom-built MATLAB simulation, thereby serving as the primary source of data for validating the proposed numerical methodology [20-23].

3. Simulation Results, Analysis and Discussions

The investigation of quantum properties and reflection phenomena was conducted using a step barrier structure, graphically represented in Figure 1. This potential configuration simulates the interaction of a quantum particle with an abrupt change in potential energy. The system models the incidence of a Gaussian wave packet with a sinusoidal carrier on a step potential energy function, $U(x)$, which is defined as:

$$U(x) = \begin{cases} 0 & for\ 0 \leq x \leq L/2 \\ U_0 & for\ L/2 \leq x \leq 0 \end{cases} \quad (9)$$

An ideal potential step serves as a robust approximation for various physical scenarios. For instance, it can model the instantaneous potential between the dees of a cyclotron when U_0 represents an attractive potential ($U_0 < 0$), or simulate the potential barrier at a metal surface when U_0 signifies a repulsive potential ($U_0 > 0$).

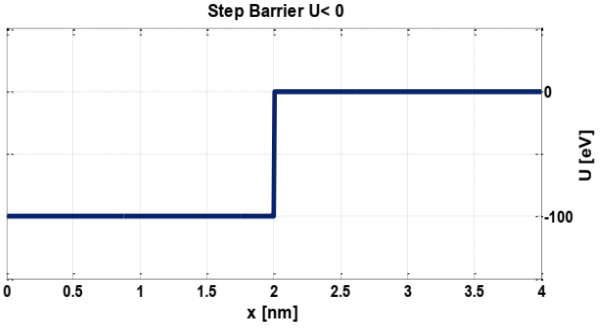

Fig. 1: A step barrier structure when $U < 0$.

Beyond the fundamental quantum mechanical properties, the developed computational framework facilitates analyzing how a system reacts to an external electric field. Graphical representations are provided to illustrate the time-evolution of the wave function and its corresponding probability density, offering visual insights into the particle's quantum behavior. Furthermore, the impact of varying electric field strengths and directions are shown for two distinct electric field configurations. The temporal evolution of the wave function ($\Psi(x, t)$) and its corresponding probability density ($|\Psi(x, t)|^2$) are graphically presented to illustrate the simulated quantum dynamics. In these figures, the initial state of the system at time $t = 0$ is consistently represented by blue curves. Conversely, the state of the particle after 10,000 computational time steps is depicted by red curves to illustrate temporal evolution. Figure 2 presents simulating an electron moving in free space and subsequently encountering an attractive potential step. This visualization depicts the particle's behavior as it transitions into a region of lower potential energy. The simulated results also, see Table 1, present the calculated values of Δx and Δp for the various quantum states investigated. These data consistently satisfy the inequality of the Heisenberg Uncertainty Principle, thereby confirming its validity within the computational framework.

Knowing that the particle is found within the system, the probability to find the particle is unity as it is given by $\psi^*(x)\psi(x)$ (the probability density function) as follows [7]:

$$\int_{-\infty}^{+\infty} \psi^*(x)\psi(x)dx = 1 \quad (10)$$

The quantity $\psi^*(x)\psi(x)$ characterizes the probability distribution for observable A. This probability demonstrates the degree to which quantum mechanics may determine the expected results when measurements are performed. The probability distribution is described by two values; the expectation value exemplifying the average value of the distribution and the uncertainty signifying the spread in values about the average.

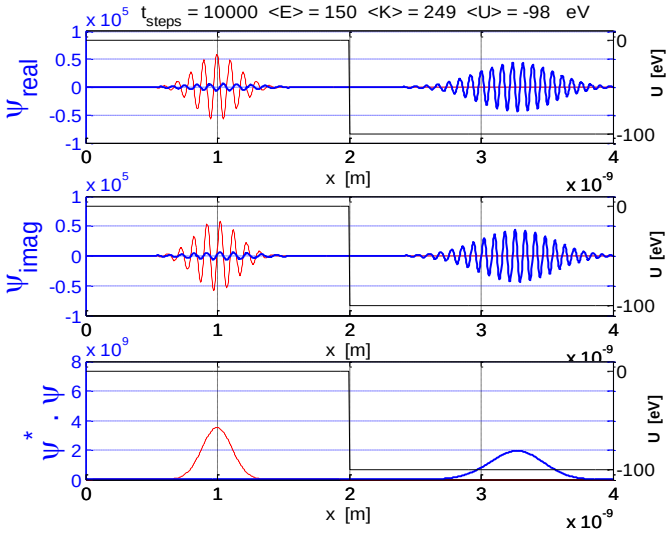

Fig. 2: Simulating the electron-wave motion in free space and then hitting an attractive potential step. The red curves for $t = 0$ and the blue ones for time after 10000 steps.

The electron is initially located in the zero-potential region with a total energy E and then propagates towards the step. A critical case investigated is when the electron's energy exceeds the potential step, specifically when $E > U_0 = -100\ eV$. Table 1 presents the key simulation results obtained for an electron interacting with this step barrier under this condition. As the wave packet moves to the right, the wave begins to spread while its kinetic energy stays the same. As the wave packet hits the barrier, part of it penetrates into the barrier whereas the other part is reflected, giving a probability of locating the electron to the left of the barrier as $P_{reflection} = 0.0171$ while the probability to locate the electron to the right of the barrier as $P_{transmission} = 0.9830$, as shown in Table 1.

Table 1: Summary of the simulation results for an electron in step barrier for $E > U_0 = -100\ eV$.

Parameter/Value	$N_t = 1000$, $N_x = 1001$
Time t [s]	2.79×10^{-16}
Probability	1.000
$P_{reflection}$	0.0171

$P_{transmission}$	0.9830
$\langle x \rangle$ [m]	3.2265 x10^{-9}
$\langle K \rangle$ [eV]	248.61
$\langle U \rangle$ [eV]	-98.27
$\langle E \rangle$ [eV]	150.34
$\langle P \rangle$ [kg.m.s]	8.169 x10^{-24}
$\langle v \rangle$[m.s^{-1}]	8.968 x10^{6}
Δx [m]	3.54 x10^{-10}
Δ p [kg.m s^{-1}]	2. 41 x10^{-24}
Δx Δp [kg.m^2 .s^{-1}]	8.55 x10^{-34}

For the case when $E > U_0 = +100\ eV$ (Fig. 3), Table 2 presents a summary of the simulation results for an electron interacting with a repulsive step barrier. This table specifically details the outcomes when the electron's total energy (E) is greater than the positive potential step ($U_0 = +100\ eV$). These results complement the analysis of the attractive potential scenario, offering further insights into the quantum particle's behaviour when encountering a barrier of higher potential energy.

Table 2: Summary of the simulation results for an electron in step barrier when $E > U_0 = +100\ eV$.

Parameter/Value	$N_t = 1000$, $N_x = 1001$
Time t [s]	2.79x10^{-16}
Probability	1.000
$P_{reflection}$	0.0939
$P_{transmission}$	0.9061
$\langle x \rangle$ [m]	2.4392 x10^{-9}
$\langle K \rangle$ [eV]	59.61
$\langle U \rangle$ [eV]	90.61
$\langle E \rangle$ [eV]	150.34
$\langle P \rangle$ [kg.m.s]	2.845 x10^{-24}
$\langle v \rangle$ [m.s^{-1}]	3.123 x10^{6}
Δx [m]	4.62 x10^{-10}
Δp [kg.m s^{-1}]	3. 06x10^{-24}
Δx Δp [kg.m^2.s^{-1}]	1.41 x10^{-33}

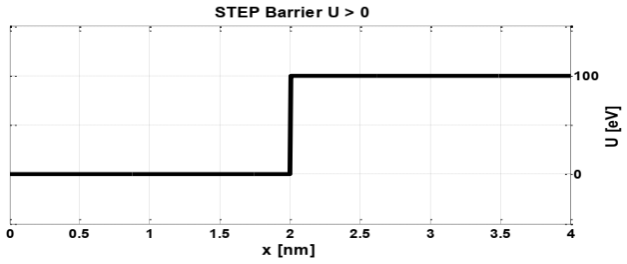

Fig. 3: Simulation of step barrier U > 0.

The energy of the electron will be all in the form of kinetic energy for the electron's motion in free space. When the electron hits the step, the potential energy expectation value increases as the kinetic energy expectation value decreases. Yet, the total energy remains conserved at all times. Noting that there exists some probability of electron reflection and some probability of penetrating the potential barrier. Simulation results in Table 2 and Fig. 4 demonstrate this eventuality.

To comprehensively understand the influence of external forces on quantum systems, the motion of an electron wave packet within a uniform electric field was also simulated. This investigation is particularly relevant for accurately estimating electric field profiles in various quantum devices. The force (F) acting on the electron within such a field is obtained directly from the potential energy function, $U(x)$, according to the fundamental relation:

$$F = -\nabla U(x) \qquad (11)$$

Given a uniform electric field, the resulting force on the electron is constant. Consequently, the potential energy function $U(x)$ adopts a linear dependence on position x, expressed in the form:

$$\mathrm{U(x)} = -\left[\frac{U_0}{L}\right] x + U_0 \qquad (12)$$

The simulations were specifically conducted for three distinct external electric field scenarios:

1. An accelerating electric field, where $U_0 > 0$, represented by a positive electric field, $E > 0$.
2. A retarding electric field, where $U_0 < 0$, represented by a negative electric field, $E < 0$.
3. A zero electric field, where $U_0 = 0$, characterized by $E = 0$ and serving as a comparative baseline.

The simulations are performed for the two cases of an accelerating and retarding electric fields; where $U_0 > 0$ for an accelerating electric field and $U_0 < 0$ for a retarding electric field. For comparison purposes, the case for zero electric field is also considered. Table 3 presents a summary of the results of three cases: (1) zero electric field $U_0 = 0$, (2) retarding electric field $U_0 = -100\ eV$ and (3) accelerating electric field $U_0 = 100\ eV$. This table consolidates the key outcomes from the three

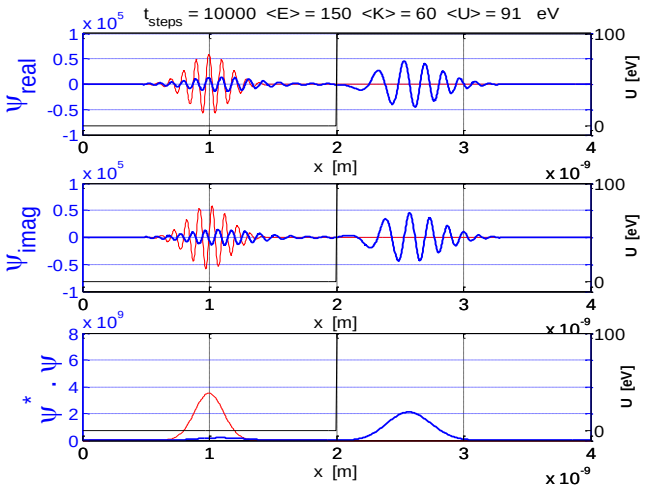

Fig. 4: The wave and probability functions simulation results. Red and blue curves as explained in Fig. 2.

cases, thereby offering a concise overview of their impact on the electron's dynamics. The results from these simulations collectively demonstrate the algorithm's capability to accurately model the particle's behaviour under various external influence.

The electric field profiles and the time evolution for the wave and probability functions for the three simulations are shown in Figs. 5-9. The number of time steps and spatial grid points used are: $N_t = 10000$ and $N_x = 1001$.

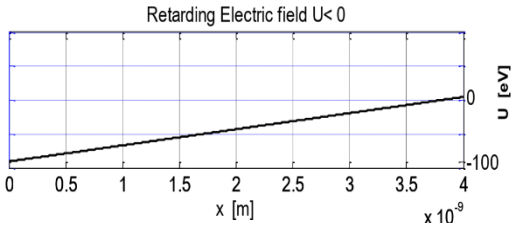

Fig. 5: Retarding electric field profile.

Table 3: Summary of electron dynamics in a uniform electric field for three cases of simulations.

Parameter/Value	Zero Field $U_0 = 0$	Retarding Field $U_0 = -100$	Accelerating Field $U_0 = 100$
Time t [s]	2.79x10^{-16}	2.79x10^{-16}	2.79x10^{-16}
Probability	1.000	1.000	1.000
$P_{reflection}$	0.000	0.000	0.000
$P_{transmission}$	1.000	1.000	1.000
$\langle x \rangle$ [m]	2.99 x x10^{-9}	2.82x10^{-9}	3.15 x10^{-9}
$\langle K \rangle$ [eV]	150.34	104.69	204.13
$\langle U \rangle$ [eV]	0.000	-29.45	21.32
$\langle E \rangle$ [eV]	150.34	75.24	225.45
$\langle P \rangle$ [kg.m.s]	6.56x10^{-24}	5.48x10^{-24}	7.62x10^{-24}
$\langle v \rangle$ [m.s^{-1}]	7.20x10^{6}	6.01x10^{6}	8.37x10^{6}
Δx [m]	1.77 x10^{-10}	1.78 x10^{-10}	1.76 x10^{-10}
Δp [kg.m.s^{-1}]	9.54 x10^{-25}	7.44 x10^{-25}	1.22 x10^{-24}
Δx Δp [kg.m^2.s^{-1}]	1.69 x10^{-34}	1.32 x10^{-34}	2.16 x10^{-34}

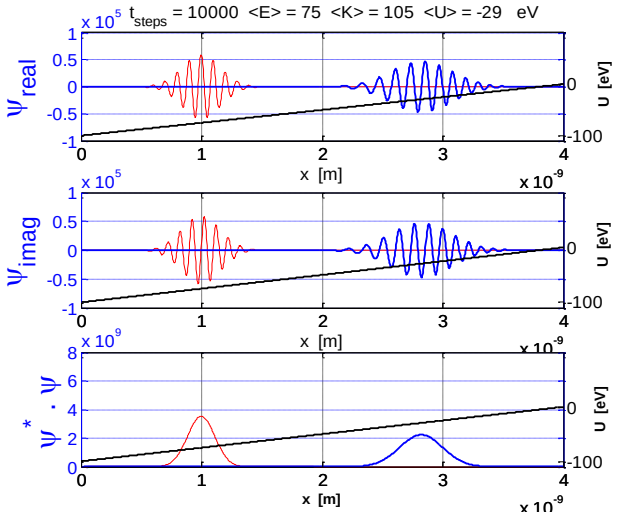

Fig. 6: The wave and probability functions simulation results for the case of retarding electric field. Red and blue curves as explained in Fig. 2.

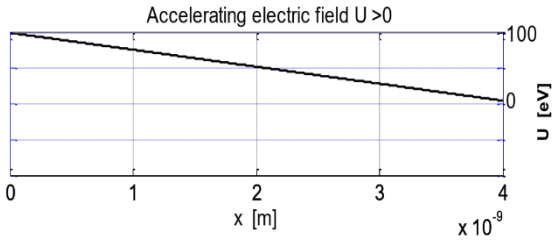

Fig. 7: Accelerating electric field profile.

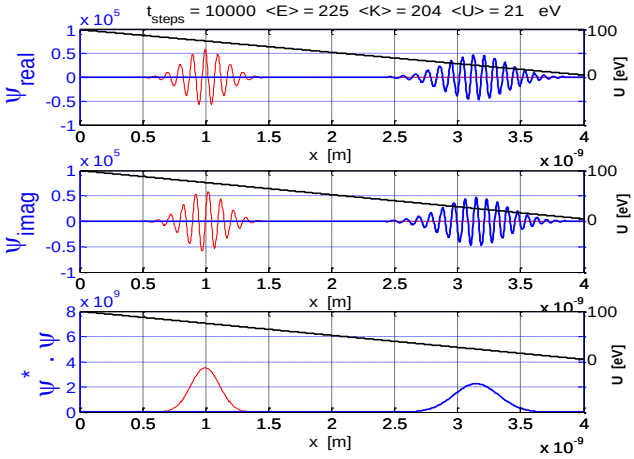

Fig. 8: The wave and probability functions simulation results for the case of an accelerating electric field. Red and blue curves as explained in Fig. 2.

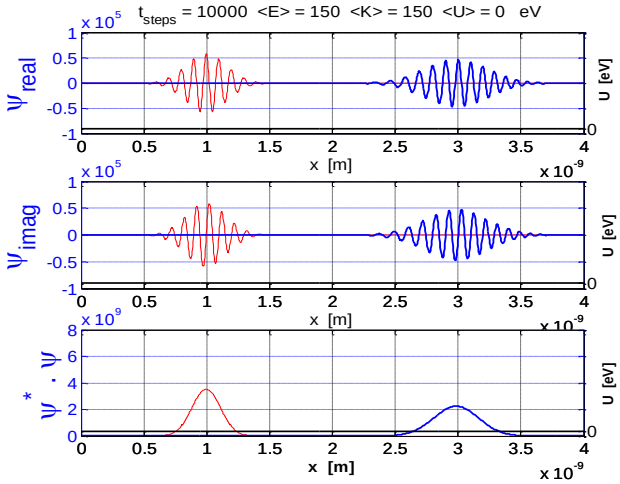

Fig. 9: The wave and probability functions simulation results for the case of zero electric field. Red and blue curves as explained in Fig. 2.

It is indicated by the findings that the classical principle of conservation of energy is also applied to the quantum system. The system's total energy is maintained as constant over time. Any increase in the kinetic energy's expectation value is balanced by an equivalent decrease in the potential energy's expectation value, and vice versa. For instance, when an electron's kinetic energy is increased by the electric force, a rise in the expectation value of kinetic energy and a corresponding drop in the expectation value of potential energy are observed, ensuring the total energy's expectation value remains unchanged. Table 4 summarizes key results from the simulated time evolution of an electron wave packet under three distinct uniform electric field conditions. The numerical parameters for these simulations were performed using a discretized grid comprising N_t = 10000 time steps and N_x = 1001 spatial grid points.

Table 4: The time evolution of electron wave packet in uniform electric fields for the three cases of simulations. The number of time steps and spatial grid points used are N_t = 10000 and N_x = 1001.

Parameter/Value	Classical Prediction		Simulation	
	Retarding Field U_0 = -100	Accelerating Field U_0 = +100	Retarding Field U_0 = -100	Accelerating Field U_0 = +100
$\langle x \rangle_{final}$ [m]	2.80 x10^{-9}	3.14 x10^{-9}	2.82x10^{-9}	3.15 x10^{-9}
$\langle v \rangle_{final}$ [m.s^{-1}]	5.91 x10^{6}	8.34x10^{6}	6.01x10^{6}	8.37x10^{6}

For the wave packet dynamics and probabilistic interpretation, as the packet propagates to the right, it exhibits spatial spreading, a characteristic quantum phenomenon often termed dispersion. Despite this dispersion, its kinetic energy remains conserved prior to interaction with the potential. Upon encountering the barrier, the incident packet undergoes partial transmission into the barrier region and partial reflection from it. This phenomenon reflects the probabilistic nature of quantum mechanics: there exists a quantifiable probability of reflection (i.e., locating the electron to the left of the barrier) and a distinct probability of transmission (i.e., finding the electron to the right of the barrier). For the simulated scenarios, the calculated probabilities, $P_{reflection}$ + $P_{transmission}$, consistently sum to approximately unity, which confirms the conservation of total probability within the system. The simulation findings unequivocally demonstrate that the classical principle of conservation of energy is robustly upheld within the quantum system. Hence, the numerical simulations performed using the Finite Difference Method (FDM) in MATLAB provide a comprehensive and accurate understanding of electron wave packet dynamics under various potential configurations. A central validation of this computational approach is its consistent adherence to fundamental quantum mechanical principles.

The observed spatial spreading, or dispersion, of the wave packet further illustrates its inherent wave-like properties. The investigations into the motion of electron wave packets in uniform electric fields provide valuable insights into how external forces influence quantum systems. A comparative analysis with classical predictions (as summarized in Table 4) allows for an understanding of the conditions under which quantum mechanical behaviour might converge towards or diverge from classical expectations. Overall, the developed FDM-based simulation provides a conceptually straightforward, accurate, and efficient tool for solving the time-dependent Schrödinger equation. Its extensibility to higher spatial dimensions and various time-dependent applications positions it as a versatile framework for exploring complex quantum phenomena, solidifying the understanding of fundamental quantum principles through computational experimentation [24-29].

4. Conclusions:

This paper successfully developed and demonstrated a robust numerical approach based on the Finite Difference Method (FDM) for solving the time-dependent Schrödinger equation (TDSE). The implemented methodology proved to be conceptually straightforward, computationally efficient, and highly accurate in modelling the dynamics of quantum particles. The simulations consistently validated fundamental quantum mechanical principles, including the Heisenberg Uncertainty Principle and the conservation of total energy (expectation value) throughout system evolution, affirming the physical integrity of the computational model. The analysis of wave packet interactions with both attractive and repulsive step barriers

provided clear insights into quantum phenomena such as wave packet dispersion, probabilistic reflection, and transmission, significantly demonstrating the conservation of total probability within the system. Furthermore, the dynamics of electron wave packets under uniform electric fields were effectively simulated, showcasing intricate energy transformations and providing valuable comparisons with classical predictions. The inherent extensibility of the FDM approach to higher spatial dimensions and its adaptability to diverse time-dependent applications underscore its versatility as a powerful tool for quantum mechanical investigations. This work significantly contributes to the computational understanding of fundamental quantum systems and lays a foundation for further research into more complex quantum phenomena or the design and analysis of quantum devices.

References

[1] Schneider, B. I. and Collins, L. A., (2005), The discrete variable method for the solution of the time-dependent Schrödinger equation, Journal of Non-Crystalline Solids, **351**(18), 1551-1558. DOI: 10.1016/j.jnoncrysol.2005.03.028

[2] Becerril, R., Guzmán, F., Rendón-Romero, A., and Valdez, S., (2008). Solving the time-dependent Schrödinger equation using finite difference methods. Revista mexicana de física E, **54**(2), 120-132.

[3] Amin, N. A., and Wong, B. R., (2015). A study of numerical solutions of the time-dependent Schrödinger equation. AIP Conference Proceedings **1682**, 020042. DOI: 10.1063/1.4932451

[4] Li, J., Li, W., Xiao, X., Liu, L., Li, Z., Ren, J., and Fang, W., (2025), Multiset Variational Quantum Dynamics Algorithm for Simulating Nonadiabatic Dynamics on Quantum Computers, Journal of Physical Chemistry Letters, ***16***(16), 3911-3919. DOI: 10.1021/acs.jpclett.5c00739

[5] Costin, O., Costin, R., Jauslin, I., and Lebowitz, J. L., (2018). Solution of the time dependent Schrödinger equation leading to Fowler-Nordheim field emission. Journal of Applied Physics, **124**(21). DOI: 10.1063/1.5066240

[6] Dubeibe, F. L., (2010), Solving the Time-Dependent SCHRÖDINGER Equation with Absorbing Boundary Conditions and Source Terms in Mathematica 6.0., International Journal of Modern Physics C, **21**(11):1391-1406. DOI: 10.1142/S0129183110015919

[7] Saad, D. Y., and Ikraiam, F. I., (2023). Simulation of Time Independent Schrödinger Equation for Finite Potential Well Using the Graphical Solution Method. Sebha University Journal of Pure and Applied Sciences, **22**(3), 236-239. DOI: 10.51984/JOPAS.V22I3.2811

[8] N. Zettili, Quantum Mechanics: Concepts and Applications, (2nd ed.) A John Wiley and Sons, Ltd., 2009.

[9] Farag, N. G. A., Eltanboly, A. H., El-Azab, M. S., and Obayya, S. S. A., (2023). Numerical Solutions of the (2+1)-Dimensional Nonlinear and Linear Time-Dependent Schrödinger Equations Using Three Efficient Approximate Schemes. Fractal and Fractional, **7**(2). DOI:10.3390/fractalfract7020188

[10] Hailin, Z., and Sun, Z., (2023). Numerical Methods for Solving the Time-Dependent Schrödinger Equation for a Molecular Dynamics Process. In book: Models and Methods for Quantum Condensation and Fluids, Lecture Notes Series. DOI: 10.1142/9789811266058_0006

[11] Adeleke, Olawale, Oke, Michael, and Adewumi, Aderemi. (2014). On a Stable and Consistent Finite Difference Scheme for a Time-Dependent Schrodinger Wave Equation in a Finitely Low Potential Well. Nigerian Journal of Basic and Applied Sciences, **22**, 51. DOI: 10.4314/njbas.v22i1.9

[12] Gao, Y., Mayfield, J., and Luo, S., (2023). Numerical solutions of the time-dependent Schrödinger equation with position-dependent effective mass. Numerical Methods for Partial Differential Equations, **39**. DOI: 10.1002/num.23006

[13] Gharibnejad, H., Schneider, B. I., Leadingham, M., and Schmale, H. J. (2020). A comparison of numerical approaches to the solution of the time-dependent Schrödinger equation in one dimension. Comput Phys Commun, **252**.

[14] Ledoux, V., and Van Daele, M., (2014). The accurate numerical solution of the Schrödinger equation with an explicitly time-dependent Hamiltonian. Computer Physics Communications, **185**(6), 1589-1594. DOI: 10.1016/j.cpc.2014.02.023

[15] Halpern, A. M., Ge, Y., and Glendening, E. D., (2022). Visualizing Solutions of the One-Dimensional Schrödinger Equation Using a Finite Difference Method. Journal of Chemical Education, **99**(8), 3053-3060. DOI: 10.1021/acs.jchemed.2c00557

[16] P. Harrison and A. Valavanis, Quantum wells, wires and dots: theoretical and computational physics of semiconductor nanostructures, John Wiley and Sons., 2016.

[17] Jennings, M., (2015). Simulation of Time-Dependent Schrödinger Equation in the Position and Momentum Domains. American Journal of Computational Mathematics, **05**, 291-303. DOI: 10.4236/ajcm.2015.53027

[18] Kabir, A., (2024). Numerical Simulation of the Time-Dependent Schrodinger Equation Using the Crank-Nicolson Method. DOI: 10.48550/arXiv.2410.10060

[19] Cooper, I., Doing Physics with MATLAB, The Time Dependent Schrodinger Equation, School of Physics, University of Sydney.

[20] Brandão, P. A., (2019). Using MATLAB to solve the linear time-dependent Schrödinger equation by the split-step Fourier method: A hands-on approach. https://www.researchgate.net/publication/337992047

[21] Los, V., and Los, N., (2013). Exact solution of the one-dimensional time-dependent Schrödinger equation with a rectangular well/barrier potential and its applications. Theoretical and Mathematical Physics, **177**. DOI: 10.1007/s11232-013-0128-8

[22] Okock, P., and Burns, T., (2015). A Matrix Method of Solving the Schrodinger Equation. DOI: 10.13140/RG.2.2.10729.83042

[23] Petridis, A. N., Staunton, L. S., Vermedahl, J., and Luban, M., (2010). Exact Analytical and Numerical Solutions to the Time-Dependent Schrödinger Equation for a One-Dimensional Potential Exhibiting Non-Exponential Decay at All Times, Journal of Modern Physics **01**(02):124-136. DOI: 10.4236/jmp.2010.12018

[24] Tong, X. M., Kato, D., Watanabe, T., and Ohtani, S., (2000). Time-dependent Schrödinger equation method: Application to charge transfer and excitation in H and H^+ collisions. Physical Review A, **62**, 052701. DOI: 10.1103/PhysRevA.62.052701

[25] van Dijk, W., (2023a). On numerical solutions of the time-dependent Schrödinger equation. American Journal of Physics, **91**(10), 826-839. DOI: 10.1119/5.0159866

[26] van Dijk, W., Brown, J., and Spyksma, K., (2011). Efficiency and accuracy of numerical solutions to the time-dependent Schrödinger equation. Physical review. E, Statistical, nonlinear, and soft matter physics, **84**, 056703. DOI: 10.1103/PhysRevE.84.056703

[27] van Dijk, W., Vanderwoerd, T., and Prins, S. J., (2017). Numerical solutions of the time-dependent Schrödinger equation in two dimensions. J. Physical Review. E., **95**, 2-1, 023310. DOI: 10.1103/PhysRevE.95.023310

[28] Wong, B., (2009). Numerical solution of the time-dependent Schrödinger equation. AIP Conference Proceedings, **1150**, 396-401. DOI: 10.1063/1.3192278

[29] Zampa, G. M., Mencarelli, D., and Pierantoni, L., (2023). A full-wave time-dependent Schrödinger equation approach for the modeling of asymmetric transport in geometric diodes. Physica B: Condensed Matter, **661**, 414917. DOI: https://doi.org/10.1016/j.physb.2023.414917